NUMERICAL COMPLEXITY OF HELIX UNRAVELING ALGORITHM FOR CHARGED PARTICLE TRACKING

Kacper Topolnicki

M. Smoluchowski Institute of Physics, Jagiellonian University
Łojasiewicza 11, 30-348 Kraków, Poland

Tomasz Bold

Department of Physics and Applied Computer Science
AGH University of Science and Technology
Reymonta 19, Kraków, Poland

*Received 2 April 2024, accepted 24 April 2024,
published online 10 May 2024*

This paper describes a procedure for estimating the number of iterations in the main loop of a recently proposed algorithm designed to detect helical charged particle tracks in detectors submerged in a magnetic field. The calculations are based on a Monte Carlo simulation of the ATLAS inner detector. The resulting estimates of numerical complexity suggest that using the new procedure for online triggering is not feasible. There are however some areas, such as triggering for particles in a specific sub-domain of the phase space, where using this procedure might be beneficial.

DOI:10.5506/APhysPolB.55.6-A1

1. Introduction

The fast and accurate recognition of helical charged particle tracks in data collected by modern colliders such as the High Luminosity LHC [1] is a crucial step in uncovering physics beyond the Standard Model. Before the start of an experiment, new methods for handling large amounts of data collected by the detector in real time and new algorithms for performing tracking [2–5] need to be considered. Particles with long lifetimes, that decay at large distances from the beam line, are of particular interest [6]. A review of methods used for particle tracking is available in [7]. The algorithm from [8] was proposed as a novel way to search for such charged particle tracks in data from high-energy physics detectors submerged in a uniform magnetic field. It is designed to be agnostic to the origin of particle tracks making it possible to detect particles with longer lifetimes.

The algorithm can be divided into independent iterations. Each individual iteration searches the collected data for helical charged particle tracks with a given set of parameters and consists of three steps:

1. Load the input data in the form of Cartesian coordinates of N detected track positions: $\mathbb{D} = \{(x_i, y_i, z_i), i = 1 \ldots N\}$.
2. Calculate the image space $\mathbb{D}' = \{u_{x_c,y_c,\nu}(x_i, y_i, z_i), i = 1 \ldots N\}$ by mapping a special function $u_{x_c,y_c,\nu}$ over $\mathbb{D}$. This function has an additional dependence on three parameters of the helix (these are discussed in more detail below): the helix axis, or center, is located at coordinates x_c, y_c and the helix pitch ν. If a helical charged particle track which matches the additional parameters of $u_{x_c,y_c,\nu}$ is present in the data collected by the detector, then these points will be mapped into a straight line along $\hat{z}$.
3. A peak detected on a $\hat{x}$–$\hat{y}$ histogram of $\mathbb{D}'$ indicates the existence of a helical particle track in $\mathbb{D}$ with parameters x_c, y_c, ν.

In these steps, N is the total number of Cartesian points from the detector and $u_{x_c,y_c,\nu}$ is a special transformation that takes a helix with given parameters x_c, y_c, ν and turns it into a straight line along $\hat{z}$ making it detectable as a histogram peak.

The three parameters of helical tracks used in the procedure are illustrated and described in Fig. 1. The explicit form of the "unraveling" function u was given in [8] as

$$u_{x_c,y_c,\nu}(x, y, z) := (x_c, y_c, 0) + R_{\hat{z}}\left(\frac{z\nu}{\sqrt{(x - x_c)^2 + (y - y_c)^2}}\right) \times ((x, y, z) - (x_c, y_c, 0)) \; . \tag{1}$$

This transformation is a rotation $R_{\hat{z}}(\alpha)$ of a Cartesian point along $\hat{z}$ with a center of rotation at (x_c, y_c) in the $\hat{x}$–$\hat{y}$ plane. What makes this transformation useful is a careful choice of the angle of rotation α. This angle depends on the $\hat{z}$ coordinate and allows the detected Cartesian points from a particle track with parameters x_c, y_c, ν to be "unraveled" into a straight line along $\hat{z}$. This collection of points can be detected as a peak on a $\hat{x}$–$\hat{y}$ histogram. In this paper, a slightly more general form of (1) is used

$$u_{x_c,y_c,\nu}(x, y, z) := (x_c, y_c, 0) + R_{\hat{z}}\left(\frac{(z - \bar{z})\nu}{\sqrt{(x - x_c)^2 + (y - y_c)^2}}\right) \times ((x, y, z) - (x_c, y_c, 0)) \; , \tag{2}$$

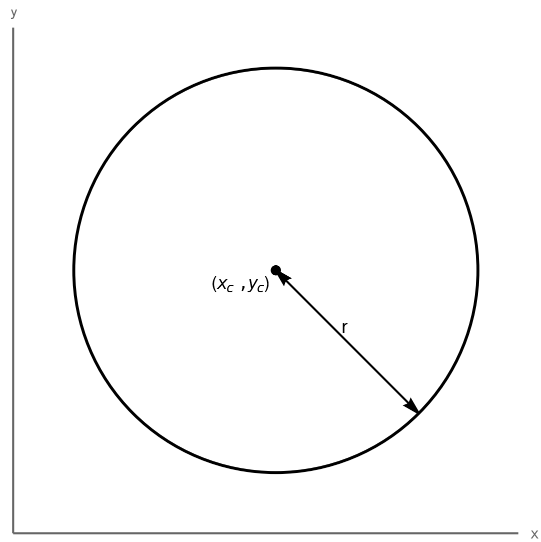

Fig. 1. A helical particle track projected on the $\hat{x}$–$\hat{y}$ plane is a circle or a fragment of a circle. The detector is centered around the origin and the beam line is perpendicular to the diagram. The helix axis, or center, position is (x_c, y_c). The third parameter ν is not illustrated and plays the role of the helix pitch. This can be seen in the explicit form of a point on the helix: $(x_c, y_c, 0) + \left(r\cos\left(-\frac{\nu(z-z_0)}{r}\right), r\sin\left(-\frac{\nu(z-z_0)}{r}\right), z\right)$, where r is the helix radius and z_0 fixes the helix's position along $\hat{z}$.

where the additional parameter $\bar{z}$ gives the flexibility to choose the fixed point of the transformation

$$u_{x_c,y_c,\nu}(x, y, \bar{z}) = (x, y, \bar{z})\,. \tag{3}$$

Setting $\bar{z} = 0$ turns (2) into (1) and results in the fixed point being on the $z = 0$ plane. This placement of the fixed point can be problematic since the $z = 0$ plane contains, in the Monte Carlo simulations used, the interaction point and may result in many peaks, close together on the $\hat{x}$–$\hat{y}$ histogram of $\mathbb{D}'$ making them difficult to distinguish. When using real data, the fixed point should be placed at a safe distance from the expected interaction point. More details about the algorithm can be found in [8].

2. Determining the step size

As mentioned in Section 1, the algorithm can be divided into independent iterations, each iteration searching the input data for tracks with a given set of parameters. In order to arrive at a full implementation of the algorithm, it is necessary to determine the change of helix parameters from one iteration to another

$$x_c, y_c, \nu \to x'_c, y'_c, \nu' \,. \tag{4}$$

The original paper [8] used an approximate approach based on dimensional analysis to determine the total number of these iterations. These results were not precise and a new approach was needed.

In this paper, we use a method based more directly on a realistic, Open Data Detector [9], Monte Carlo simulation of a detector. The following procedure is used to determine the allowable parameter step sizes:

1. Chose a reference trajectory from a random event generated by the simulation.
2. Set $\bar{z}$ to match one point on the reference trajectory. This step will make it easy to calculate the $\hat{x}-\hat{y}$ position of the "unraveled" trajectory in $\mathbb{D}'$.
3. Set the step sizes $\mathrm{d}x_c, \mathrm{d}y_c, \mathrm{d}\nu = 0, 0, 0$.
4. All parameters x_c, y_c, ν of the reference trajectory are known. Use $x_c + \mathrm{d}x_c, y_c + \mathrm{d}y_c, \nu + \mathrm{d}\nu$ to "unravel" the whole event. If the unraveling parameters do not match the reference trajectory parameters exactly, the reference helix will not unravel into a perfectly straight line.
5. Look for peaks in a bin centered at (x_c, y_c). Bin shapes and sizes are shown in Fig. 2.
6. Depending on if a peak is present or not, increase or decrease the step sizes $\mathrm{d}x_c, \mathrm{d}y_c, \mathrm{d}\nu$ accordingly. In practice, the step sizes $\mathrm{d}x_c, \mathrm{d}y_c, \mathrm{d}\nu$ are chosen to move the helix axis (x_c, y_c) in two perpendicular directions as shown in Fig. 3.
7. Repeat from 4 to determine the maximum change $\mathrm{d}x_c, \mathrm{d}y_c, \mathrm{d}\nu$ in reference trajectory helix parameters x_c, y_c, ν for which the reference trajectory is still detected.

The condition for the step size is that before and after (4) the helix is still detectable. Using this condition, the end result of the 7-step procedure above is a map of maximum allowable step sizes for different helix parameters x_c, y_c, ν. The Open Data Detector [9] simulation was also used in [8] but the simulation data was not used in estimating the numerical complexity of the algorithm.

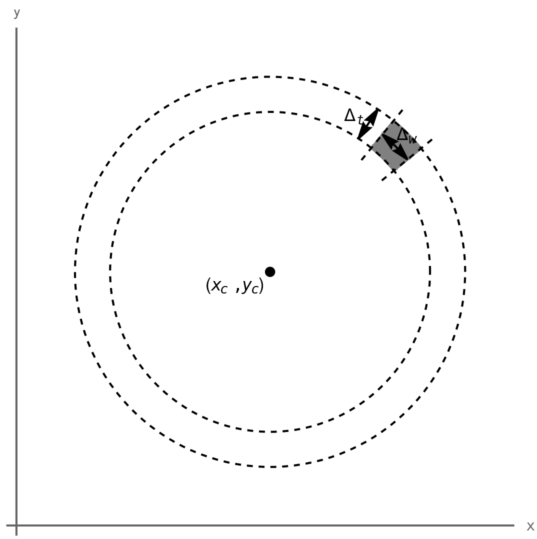

Fig. 2. The shape of bins used to determine step sizes. A single bin is a Δ_w width fragment of a round slice centered around the helix axis (x_c, y_c) with thickness Δt. In the calculations used for this paper $\Delta_w = 10^{-4}$ m and $\Delta_t = 5 \times 10^{-5}$ m. These numbers ensured that over TODO of helices were detected.

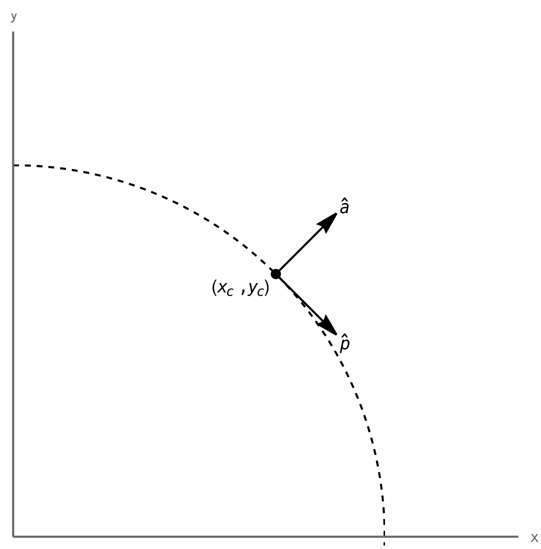

Fig. 3. When creating a map of allowable parameter changes, the helix center (x_c, y_c) was moved in two directions: along the vector from the origin $\hat{a}$ and perpendicular to this vector $\hat{p}$.

Considering the cylindrical symmetry of the detector, it can be assumed that the maximum allowable step sizes are a function of the helix axis distance from the origin r_c and the absolute value of the helix pitch $|\nu|$

$$\begin{aligned} \mathrm{d}a_c^{\max} &= \mathrm{d}a^{\max}(r_c, |\nu|)\,, \\ \mathrm{d}p_c^{\max} &= \mathrm{d}p^{\max}(r_c, |\nu|)\,, \\ \mathrm{d}\nu^{\max} &= \mathrm{d}\nu^{\max}(r_c, |\nu|)\,. \end{aligned}$$

Here, instead of using $\mathrm{d}x_c, \mathrm{d}y_c$, a shift along $\hat{a}$ and $\hat{p}$ is considered as in Fig. 3. The resulting maps are illustrated in Figs. 4–6. They can be directly used to calculate the total number of iterations in the helix detection algorithm.

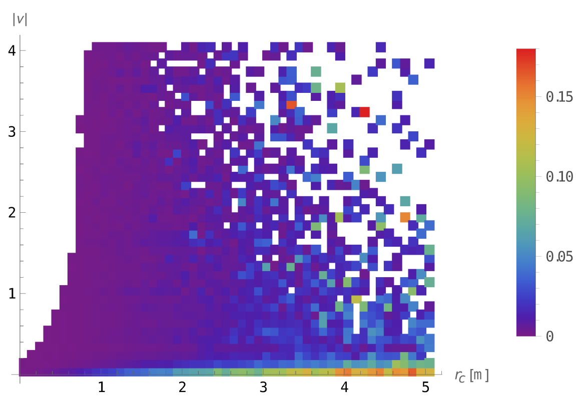

Fig. 4. Map of allowable shifts $\mathrm{d}a^{\max}(r_c, |\nu|)$, in meters, of the helix center (x_c, y_c) in the $\hat{a}$ direction from Fig. 3. The horizontal axis r_c is the distance of the helix axis from the origin. The vertical axis is the absolute value of the helix pitch ν.

The total number of iterations necessary to search for helical tracks in a region $\mathbb{G}$ of $(r_c, |\nu|)$ is

$$M_{\mathbb{G}} = 2 \int\limits_{\mathbb{G}} \frac{2\pi r_c}{\mathrm{d}p^{\max}(r_c, |\nu|)} \frac{1}{\mathrm{d}a^{\max}(r_c, |\nu|)\mathrm{d}\nu^{\max}(r_c, |\nu|)} \mathrm{d}r_c \mathrm{d}|\nu|\,. \tag{5}$$

Here,

$$\frac{2\pi r_c}{\mathrm{d}p^{\max}(r_c, |\nu|)}$$

is the number of iterations necessary for searching in the whole circle in the $\hat{p}$ direction and

$$\frac{1}{\mathrm{d}a^{\max}(r_c, |\nu|)\mathrm{d}\nu^{\max}(r_c, |\nu|)}$$

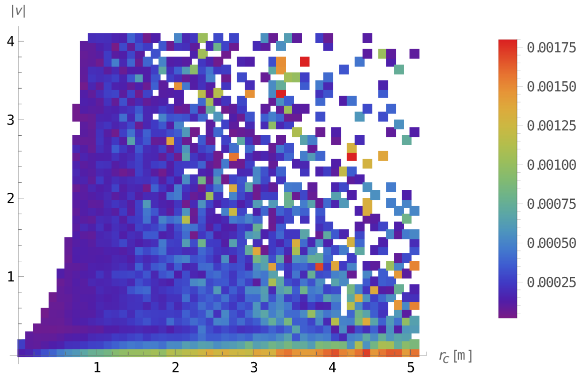

Fig. 5. Map of allowable shift $\mathrm{d}p^{\max}(r_c, |\nu|)$, in meters, of the helix center (x_c, y_c) in the $\hat{p}$ direction from Fig. 3. The horizontal axis r_c is the distance of the helix axis from the origin. The vertical axis is the absolute value of the helix pitch ν.

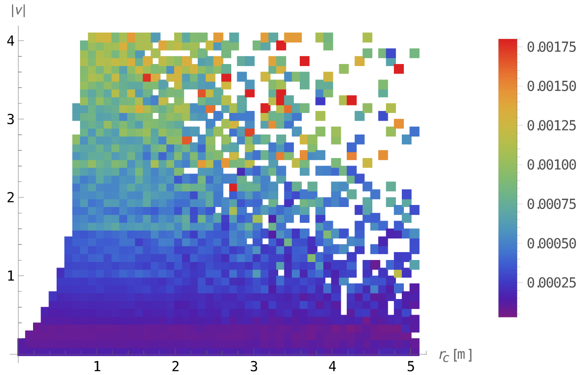

Fig. 6. Map of allowable shifts $\mathrm{d}\nu^{\max}(r_c, |\nu|)$ in the helix pitch, see Fig. 1. The horizontal axis r_c is the distance of the helix axis from the origin. The vertical axis is the absolute value of the helix pitch ν.

is the density of helix parameters in a $\mathrm{d}|\nu|$ by $\mathrm{d}r_c$ region. The product of these two quantities multiplied by $\mathrm{d}r_c\mathrm{d}|\nu|$ results in a number of iterations necessary to investigate an infinitesimal region of $(r_c, |\nu|)$. The additional factor of 2 before the integral is there to account for the helix pitch $\nu = \pm|\nu|$.

For demonstration purposes, the region $\mathbb{G}$ is chosen such that $0.1 \le |\nu| \le 1.1$ and $1.0\ \mathrm{m} \le r_c \le 2.0\ \mathrm{m}$. The numerical evaluation of the integral of (5) results in

$$M_{\mathbb{G}} \approx 1.62 \times 10^{11}\,. \tag{6}$$

In order to find all charged particle trajectories, the region $\mathbb{G}$ should be expanded making the total number of necessary iterations even larger. This unfortunately indicates that the algorithm from [8] is not a good option for triggering applications.

3. Summary and conclusions

The number of iterations necessary in order to carry out the main loop of the helix detection algorithm from [8] was estimated using a realistic Monte Carlo simulation of the ATLAS detector. Unfortunately, this indicates that the numerical complexity of the procedure is too big for triggering applications.

The Monte Carlo simulations used provide a good picture of the ATLAS detector. However, the generated events have a very small number of tracks originating away from the detector. To investigate the effect of these particles on the step size, a larger statistic is needed. Unfortunately, it is unlikely that this would have a significant effect on (6). In addition to the large numerical complexity, choosing helix parameters for the iterations would require constructing a non-uniform grid of helix parameters.

The method proposed in [8] indicates not only the existence or non-existence of a charged particle track in data collected by the detector but also gives estimates of the track's parameters. This, coupled with the algorithm being agnostic to the origin of the track, means that it might still find potential uses in data analysis for high-energy physics experiments.

REFERENCES

[1] ATLAS Collaboration (M. Arantxa Ruiz), «The ATLAS run-2 trigger menu for higher luminosities: Design, performance and operational aspects», *EPJ Web Conf.* **182**, 02083 (2018).

[2] ATLAS Collaboration (G. Aad *et al.*), «The ATLAS Experiment at the CERN Large Hadron Collider», *J. Instrum.* **3**, S08003 (2008).

[3] ATLAS Collaboration (M. Aaboud *et al.*), «Performance of the ATLAS trigger system in 2015», *Eur. Phys. J. C* **77**, 317 (2017).

[4] ATLAS Collaboration (M. Aaboud *et al.*), «Study of the material of the ATLAS inner detector for Run 2 of the LHC», *J. Instrum.* **12**, P12009 (2017).

[5] ATLAS Collaboration, «Technical Design Report for the Phase-II Upgrade of the ATLAS Trigger and Data Acquisition System — Event Filter Tracking Amendment», Technical report, CERN, Geneva, March 2022, https://cds.cern.ch/record/2802799

[6] S. Bobrovskyi, J. Hajer, S. Rydbeck, «Long-lived higgsinos as probes of gravitino dark matter at the LHC», *J. High Energy Phys.* **2013**, 133 (2013).

[7] R. Frühwirth, A. Strandlie, «Pattern Recognition, Tracking and Vertex Reconstruction in Particle Detectors», *Springer, Cham*, 1988, chapter 5.

[8] K. Topolnicki, T. Bold, «Approximate method for helical particle trajectory reconstruction in high energy physics experiments», *J. Instrum.* **17**, P08033 (2022).

[9] C. Allaire *et al.*, «OpenDataDetector», April 2022, `https://zenodo.org/records/6445359`